Tracking a CAD-ALK gene rearrangement in urine and blood of a colorectal cancer patient treated with an ALK inhibitor

Siravegna, G; Sartore-Bianchi, A; Mussolin, B; Cassingena, A; Amatu, A; Novara, L; Buscarino, M; Corti, G; Crisafulli, G; Bartolini, A; Tosi, F; Erlander, M; Di Nicolantonio, F; Siena, S; Bardelli, A. Tracking a CAD-ALK gene rearrangement in urine and blood of a colorectal cancer patient treated with an ALK inhibitor. ANNALS OF ONCOLOGY. None pp: 1-8. DOI: 10.1093/annonc/mdx095

Tracking a CAD-ALK gene rearrangement in urine and blood of a colorectal cancer patient treated with an ALK inhibitor

Giulia Siravegna[1,2,3]*, Andrea Sartore-Bianchi[4]*, Benedetta Mussolin[1]*, Andrea Cassingena[4], Alessio Amatu[4], Luca Novara[1], Michela Buscarino[1], Giorgio Corti[1], Giovanni Crisafulli[1], Alice Bartolini[1], Federica Tosi[4], Mark Erlander[5], Federica Di Nicolantonio[1,2], Salvatore Siena[4,6]* and Alberto Bardelli[1,2]*

[1]Candiolo Cancer Institute-FPO, IRCCS, 10060 Candiolo (TO), Italy; [2]Department of Oncology, University of Torino, SP 142 km 3.95, 10060 Candiolo (TO), [3] FIRC Institute of Molecular Oncology (IFOM), 20139 Milan, Italy; [4]Niguarda Cancer Center, Grande Ospedale Metropolitano Niguarda, 20162 Milan, Italy; [5]Trovagene, San Diego, CA, USA; [6] Dipartimento di Oncologia e Emato-Oncologia, Università degli Studi di Milano, 20122 Milan, Italy

*These authors contributed equally to this manuscript

Correspondence:

Salvatore Siena (salvatore.siena@ospedaleniguarda.it)

Alberto Bardelli (alberto.bardelli@unito.it)

Abstract

Background

Monitoring response and resistance to kinase inhibitors is essential to precision cancer medicine, and is usually investigated by molecular profiling of a tissue biopsy obtained at progression. However, tumor heterogeneity and tissue sampling bias limit the effectiveness of this strategy. In addition, tissue biopsies are not always feasible and are associated with risks due to the invasiveness of the procedure. To overcome these limitations, blood-based liquid biopsy analysis has proven effective to non-invasively follow tumor's clonal evolution.

Patients and methods

We exploited urine cell-free, trans-renal DNA (tr-DNA) and matched plasma circulating tumor DNA (ctDNA) to monitor a metastatic colorectal cancer patient carrying a *CAD-ALK* translocation during treatment with an ALK inhibitor.

Results

Using a custom Next Generation Sequencing (NGS) panel we identified the genomic *CAD-ALK* rearrangement and a *TP53* mutation in plasma ctDNA. Sensitive assays were developed to detect both alterations in urine tr-DNA. The dynamics of the *CAD-ALK* rearrangement in plasma and urine were concordant and paralleled patient's clinical course. Detection of *CAD-ALK* gene fusion in urine tr-DNA anticipated radiological confirmation of disease

progression. Analysis of plasma ctDNA identified *ALK* kinase mutations that emerged during treatment with the ALK inhibitor entrectinib.

Conclusion

We find that urine-based genetic testing allows tracing of tumor-specific oncogenic rearrangements. This strategy could be effectively applied to non-invasively monitor tumor evolution during therapy. The same approach could be exploited to monitor minimal residual disease after surgery with curative intent in patients whose tumors carry gene fusions. The latter could be implemented without the need of patient hospitalization since urine tr-DNA can be self-collected, is stable over time and can be shipped at specified time-points to central labs for testing.

Key words:

colorectal cancer; liquid biopsy; circulating DNA; trans-renal DNA; ALK translocation; ALK inhibitor

Key message:

A *CAD-ALK* rearrangement was tracked in urine trans-renal DNA (tr-DNA) and plasma circulating tumor DNA (ctDNA) of a metastatic colorectal cancer patient receiving treatment with an ALK inhibitor. The detection of oncogenic gene fusions in urine tr-DNA is feasible and its dynamics during treatment parallel changes observed in plasma ctDNA.

Introduction

Anaplastic lymphoma kinase (ALK) receptor is a tyrosine kinase encoded by the *ALK* gene. Gene fusion is the most frequent molecular alteration occurring in this gene across different tumor types including non-small cell lung cancer (NSCLC), leukemia, anaplastic large cell lymphoma (ALCL), inflammatory myofibroblastic tumor (IMT), and colorectal cancers (CRC) [1, 2]. *ALK* gene rearrangements lead to constitutive receptor dimerization and activation, resulting in uncontrolled tumor cell proliferation and activation of downstream MAPK and AKT pathways [3].

Recent studies have shown that plasma circulating tumor DNA (ctDNA) can be used to effectively monitor response and emergence of resistance during the course of treatment with targeted agents [4-6]. While liquid biopsies are most commonly applied to plasma-derived ctDNA, recent analyses have focused on DNA isolated from other body fluids, such as cerebrospinal fluid, saliva and urine [7-9]. It is known that a portion of blood ctDNA is cleared by the kidney barrier filtration and is excreted in urine in the form of small fragments (less than 100 bp) [10]. The applicability and clinical utility of liquid biopsies based on urine trans-renal DNA (tr-DNA) has not been extensively explored. Technical difficulties in detecting the highly fragmented and low abundant tumor-specific DNA in urine have limited progress in this field [10].

We reasoned that PCR-based assays designed to detect genetic rearrangements such as the *CAD-ALK* translocation could be used to assess the validity of urine as a source of tumor-specific genetic information. A metastatic colorectal (mCRC) patient whose tumor displayed a *CAD-ALK*

translocation showed a remarkable response during treatment with entrectinib, a potent and selective panTRK/ROS1/ALK inhibitor [11]. Here we exploited urine tr-DNA and matched blood ctDNA of this patient to monitor the *CAD-ALK o*ncogenic rearrangement during ALK blockade.

Results

Acquired resistance to ALK inhibition in a CRC patient

A molecular screen identified a 53-years-old mCRC patient with brain, thoracic lymph nodes and liver metastases carrying a *CAD-ALK* gene fusion [11]. After several rounds of standard treatments including surgery on the primary tumor (right hemicolectomy), external beam radiation therapy to the central nervous system (CNS) metastases (brain and cerebellum) and thoracic lymph nodes, and two lines of chemotherapy (both with oxaliplatin, 5-fluorouracil/leucovorin, and bevacizumab), administered before and after the radiation therapy, the patient displayed disease progression in the liver metastasis.

The patient's tumor harbored a rearrangement involving *CAD* exon 35 to *ALK* exon 20. We and others have previously reported that CRC cell models harboring *ALK* translocations are sensitive to ALK pharmacological inhibition [1, 12].

Based on this evidence, the patient was enrolled in the phase I clinical trial (EudraCT Number 2012-000148-88) of the panTRK/ROS1/ALK kinase

inhibitor entrectinib, a first-in-class drug currently undergoing clinical testing [13, 14].

The patient received entrectinib on a 400 mg/m^{-2} po qd (by mouth daily) dosing schedule. CT scans (Computed Tomography) evaluations were planned as per protocol every 8 weeks. In case of PR/CR, confirmation of response by another CT scan was mandatory after 4 weeks. At baseline in March 2015, a CT scan revealed stable and asymptomatic CNS disease (brain and cerebellum), and right and left liver lobe involvement. The treatment induced remarkable tumor shrinkage and was well tolerated, leading to a rapid partial response with a decrease in the sum of the target lesions by 38%, confirmed by a subsequent CT scan in July 2015 (Figure 1a). Brain and cerebellum metastases remained stable during the duration of the treatment**.** After 18 weeks of clinical response, drug resistance occurred, as evaluated by a CT scan in late August 2015, and the patient died in September 2015 due to progression of liver disease and hepatic failure.

Detection of *CAD-ALK* gene fusion in plasma ctDNA

To identify the *CAD-ALK* fusion genomic breakpoint, we analyzed plasma ctDNA through liquid biopsy [15], an approach we previously optimized to detect and monitor drug resistance in patients treated with targeted agents [4, 16].

ctDNA isolated from a plasma sample collected prior to treatment initiation (baseline) was subjected to molecular profiling using an NGS panel (IRCC-Fusion panel) we purposely designed to interrogate 52 common cancer gene

rearrangements (Supplementary Table 1a) and 14 frequently mutated genes in cancer patients (Supplementary Table 1b). Profiling of the pre-treatment specimen unveiled a *TP53* p.R248W mutation and detected the *CAD-ALK* gene fusion (Supplementary Table 2a), that was also present in the tumor tissue of the same individual [11].

The *ALK* rearrangement is present in urine tr-DNA and mirrors patient's response

Urine (90-110 ml of first morning void) and blood samples were longitudinally collected during treatment with the ALK inhibitor. Urine tr-DNA was isolated as described in the methods section and fragments' size distribution was evaluated using a 2100 Bioanalyzer (Supplementary Figure 1). The amount of tr-DNA extracted from the baseline urine sample (March 2015) was not sufficient to perform the analyses and was excluded (Supplementary Figure 1a).

Urine tr-DNA differs from plasma ctDNA in that there is a large amount of contaminating normal DNA shed by cells of the urinary tract in urine and consisting of high-molecular weight fragments. A standard Droplet Digital PCR (ddPCR) [17] approach failed to detect the rearrangement in tr-DNA. We reasoned that highly sensitive assays would be needed to detect the *CAD-ALK* rearrangement and the *TP53* mutation in tr-DNA. We designed several end-point PCR assays to detect the *CAD-ALK* gene fusion. We found that a 51 bp assay was optimally suited to detect the translocation in tr-DNA (Figure 1b and Supplementary Figure 2a). Using the amplicon-based assay, the

presence of the gene fusion was detectable in all urine and plasma time-points analyzed (Figure 1b and Supplementary Figure 2). The tr-DNA from an unrelated CRC patient served as a negative control. *CAD-ALK* levels increased in August 2015 when the patient showed clinical progression (Figure 1b). Of note, the *CAD-ALK* gene fusion was apparent in urine tr-DNA before radiological confirmation of progressive disease (Figure 1b and Supplementary Figure 2a). To validate the specificity of the assay we performed TOPO TA cloning of the PCR products followed by Sanger sequencing. The results confirmed the presence of the genomic rearrangement (Supplementary Figure 3).

To detect the *TP53* p.R248W variant, as an alternative marker of tumor burden and response to treatment in urine tr-DNA, peptide nucleic acid (PNA) probes were designed to specifically suppress amplification of wild-type (WT) fragments. *TP53* mutated alleles were detected in all time-points (Supplementary Figure 4).

Emergence of secondary *ALK* mutations in plasma ctDNA during entrectinib treatment

To uncover molecular alterations associated with emergence of secondary resistance to entrectinib treatment, plasma ctDNA obtained at clinical relapse was investigated with the NGS-based IRCC-TARGET panel we previously described [4]. ctDNA profiling at progression to entrectinib confirmed the presence of the *TP53* p.R248W mutation already detected in the baseline

plasma sample by the IRCC-Fusion panel NGS analysis (data not shown). Additionally, the analysis revealed five *ALK* point mutations in exons 21, 23 and 24 (p.F1174C, p.F1174L C>G and T>C, p.G1128A and p.F1245V) in the kinase domain of the protein, which were not detected in ctDNA obtained prior to entrectinib treatment (Supplementary Table 2b).

To longitudinally monitor mutant *ALK* alleles in plasma samples collected over the course of treatment, ddPCR assays were designed for individual mutations. To monitor overall disease, the *TP53* p.R248W founder mutation, as identified by NGS (Supplementary Table 2a), was also followed by ddPCR analysis in plasma ctDNA (Figure 2). Longitudinal ddPCR analysis of plasma ctDNA revealed that *ALK* mutations were initially absent (or present at very low levels) and emerged as early as 8 weeks upon initiation of treatment with entrectinib (Figure 2 and Supplementary Table 3). *ALK* mutation frequencies continued to increase in plasma ctDNA until clinical progression was radiologically confirmed (20 weeks after initiation of treatment).

Discussion

Mechanisms of resistance to targeted therapies are usually investigated by molecular profiling of a tissue biopsy obtained at progression. However, tumor heterogeneity and biases associated with tissue sampling limit the effectiveness of this strategy. In addition, tissue biopsies are not always feasible and are associated with risks due to the invasiveness of the procedure.

To address these issues we and others exploited plasma ctDNA to genotype solid tumors non-invasively and monitor clonal evolution during treatment with targeted agents [4, 6, 19-22]. However, blood draws are not exactly non-invasive and phlebotomy requires the involvement of a health professional. Furthermore, the blood volume is limited, and its collection can be impaired by health conditions and other reasons; this affects the frequency of collection, limiting patient's monitoring in real time.

In principle, these limitations can be overcome using circulating tr-DNA [23, 24]. Urine can be collected at home and there are no quantitative or timing limitations to sample collection. This may be particularly valuable in some clinical settings, for example monitoring minimal residual disease (MRD) after surgery with curative intent. In this situation, one can envision the patient collecting urine at home over several days (weeks) followed by centralized analyses of trans-renal DNA aimed at identification of cancer specific alterations to determine MRD. We also note that recent evidence indicates that urine tr-DNA analysis can reach remarkable sensitivity when using appropriate sample volumes [7, 25].

Only a limited number of studies have exploited DNA extracted from urine for the molecular characterization of cancer patients [7, 26-29]. Concordance among somatic mutations detected in matched tumor tissue, plasma, and urine has been reported [7, 30]. These reports include *KRAS* mutations in CRC, *BRAF* mutations in histiocytic disorders and *EGFR* mutations in NSCLC [7, 27]. Several causes have limited the use of tr-DNA as a source of tumor-

specific genomic information. For example, it is currently unclear what fraction of cancer patients carries tumor-derived DNA fragments in urine. Another limitation to the use of tr-DNA is that tumor DNA represents a very low fraction of the total tr-DNA, and therefore detection assays must be highly sensitive. We reasoned that oncogenic rearrangements (gene fusions) would be uniquely suited for urine-based assays since PCR reactions spanning somatically rearranged loci are not influenced by the presence of wild-type DNA that is found in large amounts in tr-DNA.

To provide proof of concept that this approach is feasible, we studied urine tr-DNA and matched plasma ctDNA of a patient with a *CAD-ALK* rearranged metastatic colorectal cancer who received the ALK kinase inhibitor, entrectinib. Our findings suggest that detection of gene fusions in urine tr-DNA is feasible and that its dynamics during treatment with a targeted agent parallel changes observed in plasma ctDNA.

Sequencing plasma ctDNA further revealed that during entrectinib treatment several *ALK* mutations (p.F1174C, p.F1174L, p.F1245V and p.G1128A) emerged. These variants were reported in both familial and sporadic neuroblastoma [31-34] and were also functionally linked to secondary resistance to other ALK inhibitors in NSCLC, as well as in neuroblastoma [32, 35-37]. p.F1174 is one of the most common hotspot mutations in exon 23, which is located at the end of the kinase domain C-helix [3], with the occurrence of p.F1174L and the p.F1174C alterations being the most and least frequent, respectively (37% and 4% among *ALK* mutant

neuroblastomas) [31]. The p.G1128A mutation (exon 21) was found in neuroblastoma, and it is located in the glycine-rich P loop, generating a gain of function kinase [3, 38]. Although the mechanism of activation is not clear, this mutation presumably alters interaction of the kinase domain with ATP increasing phosphate transfer. The *ALK* p.F1245V mutation in exon 24, previously observed in sporadic neuroblastoma [3], is located in the tyrosine kinase domain, and corresponds to the L833 residue of EGFR, a mutation which is associated with gefitinib resistance in lung cancer [32]. Mutations occurring at codons 1174 and 1245 have a strong effect on ALK receptor auto-phosphorylation due to the destabilization of ALK's auto inhibitory interaction and promotion of tyrosine kinase domain activation [38]. Of note, p.F1174L mutation that we detected at resistance to entrectinib is sensitive to second-generation ALK inhibitors such as alectinib and TAE684 [32, 39]. Similarly, ASP3026 displays activity against the activating ALK mutants F1174L and R1275Q and against the crizotinib-resistant gatekeeper mutation L1196M [40]. Our data suggest that additional lines of therapy based on already available ALK inhibitors could be administered concomitantly to prevent or overcome the emergence of resistance.

In summary, we find that urine-based genetic testing allows the tracing of tumor-specific oncogenic rearrangements. This strategy could be effectively applied to non-invasively monitor tumor evolution during therapy. The same approach could also be employed to monitor minimal residual disease after surgery with curative intent in patients whose tumors carry gene fusions. The latter do not require patient hospitalization since urine DNA can be self-

collected, is stable over time and can be shipped to central labs for testing [23].

This study provides proof of concept that trans-renal DNA can be effective in monitoring tumor evolution. The approach should now be validated in large number of patients.

This study assessed a limited number of genetic variants in tr-DNA, in the future NGS approaches will likely provide a more comprehensive landscape of trans-renal DNA. While the analysis of trans-renal tumor DNA are presently complex and limited by sensitivity, advances on DNA sequencing technologies will likely overcome current limitations.

Acknowledgements

We thank Pamela Arcella, Monica Montone and Simona Lamba for technical support with the experiments. This study was supported by European Community's Seventh Framework Programme under grant agreement no. 602901 MErCuRIC (A.B. and F.D.N.); H2020 grant agreement no. 635342-2 MoTriColor (A.B. and S.S.); IMI contract n. 115749 CANCER-ID (A.B.); AIRC 2010 Special Program Molecular Clinical Oncology 5 per mille, Project n. 9970 (A.B. and S.S.); Fondazione Piemontese per la Ricerca sul Cancro-ONLUS 5 per mille 2011 Ministero della Salute (A.B.); AIRC IG n. 16788 (A.B.); Grant Terapia Molecolare Tumori from Fondazione Oncologia Onlus (A.S-B. and S.S.); Grant Ricerca Finalizzata 2009 Identification and monitoring of gene mutations in peripheral blood and urine as a diagnostic

tool for patients with solid tumors from Ministero Salute and Regione Lombardia (S.S.).

Competing interests statement

A.B. is a member of the scientific advisory board for Trovagene. M.E. is an employee and member of the board of directors of Trovagene. All other authors declare no conflicts of interests.

Material and Methods

Patient's case report

The patient received treatment with entrectinib 400 mg/m^2 2 po qd within the ALKA-372-001 phase I study (EudraCT Number: 2012-000148-88) for which she provided informed consent. Objective tumor response was measured by computed tomography (CT) using the Response Evaluation Criteria in Solid Tumors (RECIST version 1.1) [41]. Patient's urine and plasma samples were obtained through study protocols approved by the Ethical Committee at Ospedale Niguarda, Milan, Italy.

Plasma and urine Samples Collection

At least 10 mL of whole blood were collected by blood draw using EDTA as anticoagulant. Plasma was separated within 5 hours through 2 different centrifugation steps (the first at room temperature for 10 minutes at 1,600 × g

and the second at 3,000 × g for the same time and temperature), obtaining up to 3 mL of plasma. Plasma was stored at -80°C until ctDNA extraction.

Urine samples, between 50-110 mL, were collected in the clinic into 120- mL cups, supplemented with preservative, and stored at or below -70°C.

ctDNA and tr-DNA isolation from plasma and urine

ctDNA was extracted from plasma using the QIAamp Circulating Nucleic Acid Kit (Qiagen) according to the manufacturer's instructions.

For urinary DNA extraction, urine was concentrated to 4 mL using Vivacell 100 concentrators (Sartorius Corp) and incubated with 700 µl of Q-sepharose Fast Flow quaternary ammonium resin (GE Healthcare). Tubes were spun to collect sepharose and bound DNA. The pellet was re-suspended in a buffer containing guanidinium hydrochloride and isopropanol, and the eluted DNA was collected as a flow-through using polypropylene chromatography columns (Bio-Rad). The DNA was further purified using Qia-Quick columns (Qiagen). tr-DNA fragment size distribution was assessed using the 2100 Bioanalyzer High-Sensitivity DNA assay kit (Agilent Technologies) according to the manufacturer's instructions.

Droplet Digital PCR analysis

Isolated circulating free DNA was amplified using ddPCR™ Supermix for Probes (Bio-Rad) with *ALK* p.F1174C, p.F1174L (C>G and T>C), p.G1128A, p.F1245V and *TP53* p.R248W assays (custom designed probes). ddPCR was then performed according to the manufacturer's protocol and the results were

reported as percentage or fractional abundance of mutant DNA alleles to total (mutant plus wild type) DNA alleles.

8–10 µl of DNA template was added to 10 µl of ddPCR Supermix for Probes (Bio-Rad) and 2 µl of the primer and probe mixture. Droplets were generated using Auto-DG where the reaction mix was added together with Droplet Generation Oil for Probes (Bio-Rad). Droplets were then transferred to a 96-well plate (Eppendorf) and then thermal cycled with the following conditions: 5 minutes at 95°C, 40 cycles of 94°C for 30s, 55°C for 1 minute followed by 98°C for 10 minutes (Ramp Rate 2°C/sec). Droplets were analyzed with the QX200 Droplet Reader (Bio-Rad) for fluorescent measurement of FAM and HEX probes. Gating was performed based on positive and negative controls, and mutant populations were identified. The ddPCR data were analyzed with QuantaSoft analysis software (Bio-Rad) to obtain fractional abundance of the mutated alleles in the wild-type or normal background. The quantification of the target molecule was presented as number of total copies (mutant plus WT) per sample in each reaction. The number of positive and negative droplets is used to calculate the concentration of the target and reference DNA sequences and their Poisson-based 95% confidence intervals, as previously shown [42]. ddPCR analysis of normal control DNA (from cell lines) and no DNA template controls were always included. Samples with too low positive events were repeated at least twice in independent experiments to validate the obtained results.

End-point PCR analysis

End-point PCR was performed as follows: ctDNA and tr-DNA with 0.05 U of platinum Taq DNA polymerase (Invitrogen), 1X platinum buffer (Invitrogen), 1 mM dNTPs (Invitrogen), 1.5 mM MgCl2 (Invitrogen), 1 µM of each primer was amplified using the following cycling conditions: 1 cycle of 98 °C for 2 min; 3 cycles of 98 °C for 10 s, 68 °C for 15 s, 72 °C for 15 s; 3 cycles of 98 °C for 10 s, 65 °C for 15 s, 72 °C for 15 s; 3 cycles of 98 °C for 10 s, 63 °C for 15 s, 72 °C for 15 s; 41 cycles of 98 °C for 10 s, 57 °C for 15 s, 72 °C for 15 s. Specific ultra-short primer pairs (51 bp amplicon) were used. Primer sequences are available upon request. 4% Agarose gel electrophoresis was subsequently performed with E-Gel® 1 Kb Plus DNA Ladder (Thermo Fisher Scientific). Bands of interest were quantified by Image J software (NIH Image, NIH Bethesda, USA). Calculation was done by subtracting the background intensity (calculated by measuring the intensity of an area which does not have any bands in chemiluminescent film) from intensity of the band of interest.

TOPO TA cloning and Sanger Sequencing

CAD-ALK specific amplicon obtained by end-point PCR performed on gDNA obtained from the PDX (positive control), plasma ctDNA and urine tr-DNA were cloned in TOP10 competent cells using the TOPO® TA Cloning® Kit for Sequencing (Life Technologies) according to the manufacturer's protocol. Samples were then subjected to automated sequencing by ABI PRISM 3730 (Applied Biosystems) with M13 reverse primer.

Peptide nucleic acids (PNA) assays

Peptide nucleic acid (PNA)-mediated clamped PCR was performed as follows: tr-DNA with 0.05 U of platinum Taq DNA polymerase (Invitrogen), 1X platinum buffer (Invitrogen), 1 mM dNTPs (Invitrogen), 1.5 mM MgCl2 (Invitrogen), 1 μM of each primer and 35 nM of custom designed *TP53* codon 248 PNA (NH2-TGAACCGGAGGCCCATCC-CONH2) was amplified with the following conditions: 5 minutes at 95°C, 40 cycles of 94°C for 30 s, 85°C for 30 s, 55°C for 1 minute followed by 98°C for 10 minutes (Ramp Rate 2°C/sec). Bands were quantified as per End-Point PCR procedure above.

IRCC-Fusion and IRCC-TARGET Next Generation Sequencing panels

IRCC-Fusion panel was designed selecting the most recurrent seven kinase fusions in cancer. For all of them the most frequent rearrangement partners were identified. Capture probes were designed exploiting the tool available online (https://designstudio.illumina.com), covering the exon and intron of the upstream 5' and the downstream 3' partner (Supplementary table 1a).

The panel also covers: hot-spot mutations previously associated to resistance to EGFR blockade in CRC (*KRAS*, *NRAS*, *BRAF*, *PIK3CA*, *MAP2K1*, *EGFR*); promoter of the epidermal growth factor receptor (EGFR) ligands; all coding exons of four genes known to be involved in CRC tumorigenesis (*PTEN*, *TP53*, *APC*, *CTNNB1*) (Supplementary table 1b).

Libraries were prepared with Nextera Rapid Capture Custom Enrichment Kit (Illumina Inc., San Diego, CA, USA), according to the manufacturer's protocol. Libraries preparation was performed using up to 150ng of plasma ctDNA with NEBNext® Ultra™ DNA Library Prep Kit for Illumina® (New England BioLabs

Inc., Ipswich MA), with optimized protocol. ctDNA was then used as template for indexing PCR which allows the introduction of unique sample barcodes. DNA fragments' size distribution was assessed using the 2100 Bioanalyzer with the High Sensitivity DNA assay kit (Agilent Technologies, Santa Clara, CA). Equal amount of DNA libraries were pooled and subjected to targeted panel hybridization capture. Libraries were then sequenced on the Illumina MiSeq sequencer (Illumina Inc., San Diego, CA, USA). Full description of IRCC-TARGET panel can be found in [5].

Bioinformatic Analysis

To detect the *CAD-ALK* rearrangement, a mix of BWA [44] and BLAT [45] was used. Reads were first aligned with BWA to the hg19 human reference genome. Afterwards, reads that were not perfectly aligned by BWA, potentially harboring translocations, were further processed using BLAT (tileSize=11, stepSize=5). The resulting PSL alignment was post-processed with a custom built script to detect alignments supporting translocations events. Gene fusion calling was performed according to the following criteria: each fusion partner must have at least 25 nucleotides mapped to the respective part of the read; the fusion partners must map to two different genes; each fusion breakpoint must be supported by at least 10 reads.

To detect somatic variation, FastQ files generated by Illumina MiSeq were mapped to the human reference (assembly hg19) using BWA-mem algorithm [44]. Sequences were then processed to remove all bases in the read with a Phred quality score less than 20. PCR duplicates were removed using the SAMtools package [46]. Somatic variations were called according to

previously published methods [5]. A mutational analysis with IRCC-TARGET panel was performed comparing the pre- and post- treatment samples; with Mini-Fusion panel, the human genome (hg19) was used as reference to call somatic variations. Mutations were annotated printing out gene information, number of normal and mutated reads, allelic frequencies, variation effect and the association of each hit with the corresponding number of occurrences in the COSMIC database [47].

Figure legends

Figure 1

Monitoring *CAD-ALK* rearrangement in patient's plasma ctDNA and urine tr-DNA (a) CT scans of a mCRC patient harboring a *CAD-ALK* rearrangement were recorded at baseline (March 2015), at the time of partial response (July 2015) and upon disease progression to the panTRK/ROS1/ALK inhibitor entrectinib (August 2015). **(b)** Longitudinal analysis of plasma ctDNA collected at different time-points throughout the treatment. Black and red bars: absolute CAD-ALK fragments intensity measured by end-point PCR performed on plasma and urine samples respectively.

Figure 2

Monitoring tumor evolution in patient's plasma ctDNA through ddPCR analysis

Longitudinal analysis of plasma ctDNA collected at different time-points throughout the treatment. Black line: *TP53* mutated alleles (%); grey, purple, green, red and blue lines: *ALK* mutated alleles (%). PR: partial response; PD: progressive disease

Supplementary Figure 1

Bioanalyzer High-Sensitivity DNA chip electropherograms

(a-f) panels show tr-DNA fragments size distribution assessed using the 2100 Agilent Bioanalyzer High-Sensitivity DNA assay kit.

Supplementary Figure 2

Top panels: 4% agarose gel electrophoresis showing *CAD-ALK* specific amplicons from urine tr-DNA (**a**) and plasma ctDNA (**b**) obtained by end-point PCR.

Bottom panels: peaks area obtained by measuring gel bands intensity of *CAD-ALK* gene fusion alleles observed in urine tr-DNA (**a**) and plasma ctDNA (**b**) using Image J software.

Supplementary Figure 3

Sanger sequencing electropherograms showing the *CAD-ALK* genomic break-point region obtained through TOPO TA cloning of the end-point PCR

amplicon obtained from patient's tumor tissue (patient-derived xenograft: PDX) used as positive control and from plasma ctDNA and urine tr-DNA (August 28th time-point).

Supplementary Figure 4

Tracking *TP53* mutation in urine tr-DNA

(a) 4% agarose gel electrophoresis showing mutant *TP53* p.R248W specific amplicons from urine tr-DNA obtained by PNA-clamp PCR. **(b)** Absolute quantification of *TP53* p.R248W bands intensity in urine tr-DNA exploiting PNA-clamp PCR.

Supplementary Table 1

IRCC-Fusion NGS genes panel used to analyze ctDNA

Description of the IRCC-Fusion panel. **(a)**: list of kinases selected for fusion detection and their more frequent partners. **(b)**: list of genes selected for mutational analysis.

Supplementary Table 2

NGS analysis of ctDNA collected before treatment initiation and at clinical relapse

(a) *TP53* p.R248W founder mutation and the *CAD-ALK* rearrangement found in the patient's plasma ctDNA obtained before initiation of entrectinib using the IRCC-Fusion Next Generation Sequencing panel.

(b) Five activating *ALK* mutations that emerged in patient's plasma ctDNA at acquired resistance to entrectinib as identified by IRCC-TARGET panel. nonsyn: non synonymous;

Supplementary Table 3

ddPCR raw data of longitudinal analysis of plasma ctDNA

The table lists the ddPCR events obtained analyzing longitudinal ctDNA samples. Each experiment was performed at least in triplicate.

References

1. Medico E, Russo M, Picco G et al. The molecular landscape of colorectal cancer cell lines unveils clinically actionable kinase targets. Nat Commun 2015; 6: 7002.
2. Chiarle R, Voena C, Ambrogio C et al. The anaplastic lymphoma kinase in the pathogenesis of cancer. Nat Rev Cancer 2008; 8: 11-23.
3. Hallberg B, Palmer RH. Mechanistic insight into ALK receptor tyrosine kinase in human cancer biology. Nat Rev Cancer 2013; 13: 685-700.
4. Siravegna G, Mussolin B, Buscarino M et al. Clonal evolution and resistance to EGFR blockade in the blood of colorectal cancer patients. Nat Med 2015; 21: 795-801.
5. Russo M, Siravegna G, Blaszkowsky LS et al. Tumor heterogeneity and lesion-specific response to targeted therapy in colorectal cancer. Cancer Discov 2015.
6. Siravegna G, Marsoni S, Siena S, Bardelli A. Integrating liquid biopsies into the management of cancer. Nature Reviews Clinical Oncology 2017.
7. Reckamp KL, Melnikova VO, Karlovich C et al. A Highly Sensitive and Quantitative Test Platform for Detection of NSCLC EGFR Mutations in Urine and Plasma. J Thorac Oncol 2016.
8. Wang Y, Springer S, Mulvey CL et al. Detection of somatic mutations and HPV in the saliva and plasma of patients with head and neck squamous cell carcinomas. Sci Transl Med 2015; 7: 293ra104.
9. De Mattos-Arruda L, Mayor R, Ng CK et al. Cerebrospinal fluid-derived circulating tumour DNA better represents the genomic alterations of brain tumours than plasma. Nat Commun 2015; 6: 8839.
10. Melkonyan HS, Feaver WJ, Meyer E et al. Transrenal nucleic acids: from proof of principle to clinical tests. Ann N Y Acad Sci 2008; 1137: 73-81.
11. Amatu A, Somaschini A, Cerea G et al. Novel CAD-ALK gene rearrangement is drugable by entrectinib in colorectal cancer. Br J Cancer 2015; 113: 1730-1734.
12. Lipson D, Capelletti M, Yelensky R et al. Identification of new ALK and RET gene fusions from colorectal and lung cancer biopsies. Nat Med 2012; 18: 382-384.
13. Drilon A, De Braud F, Siena S et al. Abstract CT007: Entrectinib, an oral pan-Trk, ROS1, and ALK inhibitor in TKI-naïve patients with advanced solid tumors harboring gene rearrangements: Updated phase I results. In AACR Annual meeting. New Orleans (LA): 2016.
14. Drilon AS, Salvatore, Ou S-HP, Manish Ahn, Myung-Ju, Lee JB, Todd et al. Safety and Antitumor Activity of the Multi-Targeted Pan-TRK, ROS1, and ALK Inhibitor Entrectinib (RXDX-101): Combined Results from Two Phase 1 Trials Cancer Discovery 2016.
15. Siravegna G, Bardelli A. Genotyping cell-free tumor DNA in the blood to detect residual disease and drug resistance. Genome Biol 2014; 15: 449.
16. Russo M, Misale S, Wei G et al. Acquired Resistance to the TRK Inhibitor Entrectinib in Colorectal Cancer. Cancer Discov 2016; 6: 36-44.
17. Reinert T, Schøler LV, Thomsen R et al. Analysis of circulating tumour DNA to monitor disease burden following colorectal cancer surgery. Gut 2015.

18. Hindson BJ, Ness KD, Masquelier DA et al. High-throughput droplet digital PCR system for absolute quantitation of DNA copy number. Anal Chem 2011; 83: 8604-8610.
19. Murtaza M, Dawson SJ, Tsui DW et al. Non-invasive analysis of acquired resistance to cancer therapy by sequencing of plasma DNA. Nature 2013; 497: 108-112.
20. Gremel G, Lee RJ, Girotti MR et al. Distinct sub-clonal tumour responses to therapy revealed by circulating cell-free DNA. Ann Oncol 2016.
21. Heitzer E, Auer M, Hoffmann EM et al. Establishment of tumor-specific copy number alterations from plasma DNA of patients with cancer. Int J Cancer 2013; 133: 346-356.
22. Bettegowda C, Sausen M, Leary RJ et al. Detection of circulating tumor DNA in early- and late-stage human malignancies. Sci Transl Med 2014; 6: 224ra224.
23. Umansky SR, Tomei LD. Transrenal DNA testing: progress and perspectives. Expert Rev Mol Diagn 2006; 6: 153-163.
24. Botezatu I, Serdyuk O, Potapova G et al. Genetic analysis of DNA excreted in urine: a new approach for detecting specific genomic DNA sequences from cells dying in an organism. Clin Chem 2000; 46: 1078-1084.
25. Fujii T, Barzi A, Sartore-Bianchi A et al. Mutation-Enrichment Next-Generation Sequencing for Quantitative Detection of KRAS Mutations in Urine Cell-Free DNA from Patients with Advanced Cancers. Clin Cancer Res 2017.
26. Casadio V, Calistri D, Salvi S et al. Urine cell-free DNA integrity as a marker for early prostate cancer diagnosis: a pilot study. Biomed Res Int 2013; 2013: 270457.
27. Hyman DM, Diamond EL, Vibat CR et al. Prospective blinded study of BRAFV600E mutation detection in cell-free DNA of patients with systemic histiocytic disorders. Cancer Discov 2015; 5: 64-71.
28. Su YH, Wang M, Brenner DE et al. Detection of mutated K-ras DNA in urine, plasma, and serum of patients with colorectal carcinoma or adenomatous polyps. Ann N Y Acad Sci 2008; 1137: 197-206.
29. Klempner SJ, Gershenhorn B, Tran P et al. BRAFV600E Mutations in High-Grade Colorectal Neuroendocrine Tumors May Predict Responsiveness to BRAF-MEK Combination Therapy. Cancer Discov 2016; 6: 594-600.
30. Hoque MO, Begum S, Topaloglu O et al. Quantitative detection of promoter hypermethylation of multiple genes in the tumor, urine, and serum DNA of patients with renal cancer. Cancer Res 2004; 64: 5511-5517.
31. Chen Y, Takita J, Choi YL et al. Oncogenic mutations of ALK kinase in neuroblastoma. Nature 2008; 455: 971-974.
32. George RE, Sanda T, Hanna M et al. Activating mutations in ALK provide a therapeutic target in neuroblastoma. Nature 2008; 455: 975-978.
33. Janoueix-Lerosey I, Lequin D, Brugières L et al. Somatic and germline activating mutations of the ALK kinase receptor in neuroblastoma. Nature 2008; 455: 967-970.
34. Mossé YP, Laudenslager M, Longo L et al. Identification of ALK as a major familial neuroblastoma predisposition gene. Nature 2008; 455: 930-935.
35. Katayama R, Shaw AT, Khan TM et al. Mechanisms of acquired crizotinib resistance in ALK-rearranged lung Cancers. Sci Transl Med 2012; 4: 120ra117.

36. Sasaki T, Okuda K, Zheng W et al. The neuroblastoma-associated F1174L ALK mutation causes resistance to an ALK kinase inhibitor in ALK-translocated cancers. Cancer Res 2010; 70: 10038-10043.
37. Gainor JF, Dardaei L, Yoda S et al. Molecular Mechanisms of Resistance to First- and Second-Generation ALK Inhibitors in ALK-Rearranged Lung Cancer. Cancer Discov 2016; 6: 1118-1133.
38. Bresler SC, Weiser DA, Huwe PJ et al. ALK mutations confer differential oncogenic activation and sensitivity to ALK inhibition therapy in neuroblastoma. Cancer Cell 2014; 26: 682-694.
39. McDermott U, Iafrate AJ, Gray NS et al. Genomic alterations of anaplastic lymphoma kinase may sensitize tumors to anaplastic lymphoma kinase inhibitors. Cancer Res 2008; 68: 3389-3395.
40. Awad MM, Shaw AT. ALK inhibitors in non-small cell lung cancer: crizotinib and beyond. Clin Adv Hematol Oncol 2014; 12: 429-439.
41. Eisenhauer EA, Therasse P, Bogaerts J et al. New response evaluation criteria in solid tumours: revised RECIST guideline (version 1.1). Eur J Cancer 2009; 45: 228-247.
42. Zhang L, Ridgway LD, Wetzel MD et al. The identification and characterization of breast cancer CTCs competent for brain metastasis. Sci Transl Med 2013; 5: 180ra148.

Figure 1

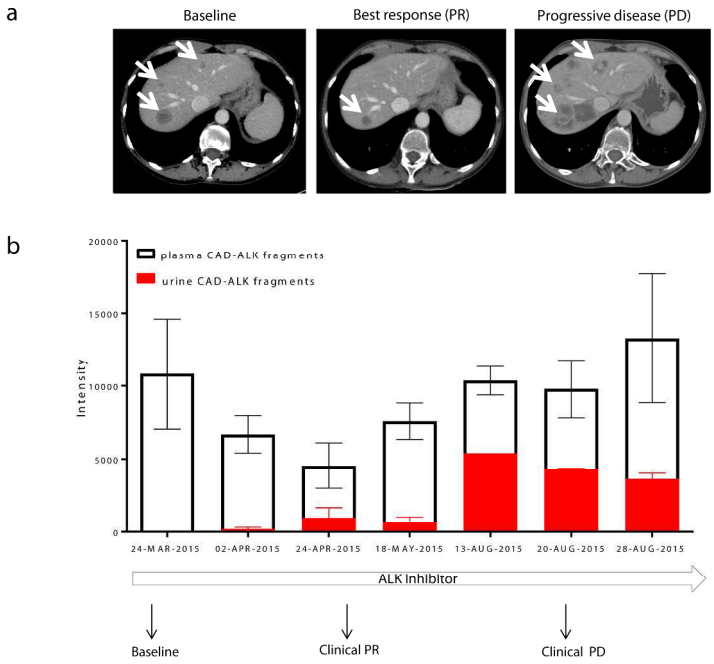

Figure 1
Monitoring CAD-ALK rearrangement in patient's plasma ctDNA and urine tr-DNA (a) CT scans of a mCRC patient harboring a CAD-ALK rearrangement were recorded at baseline (March 2015), at the time of partial response (July 2015) and upon disease progression to the panTRK/ROS1/ALK inhibitor entrectinib (August 2015). (b) Longitudinal analysis of plasma ctDNA collected at different time-points throughout the treatment. Black and red bars: absolute CAD-ALK fragments intensity measured by end-point PCR performed on plasma and urine samples respectively.

254x190mm (300 x 300 DPI)

Figure 2

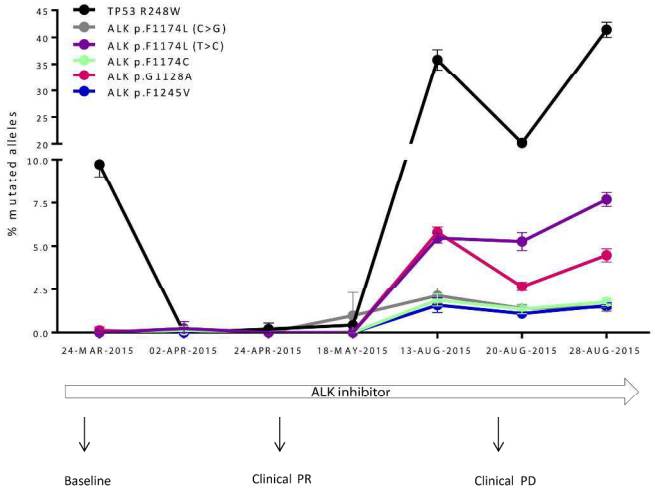

Figure 2
Monitoring tumor evolution in patient's plasma ctDNA through ddPCR analysis
Longitudinal analysis of plasma ctDNA collected at different time-points throughout the treatment. Black line: TP53 mutated alleles (%); grey, purple, green, red and blue lines: ALK mutated alleles (%). PR: partial response; PD: progressive disease

254x190mm (300 x 300 DPI)

Supplementary Figure 1

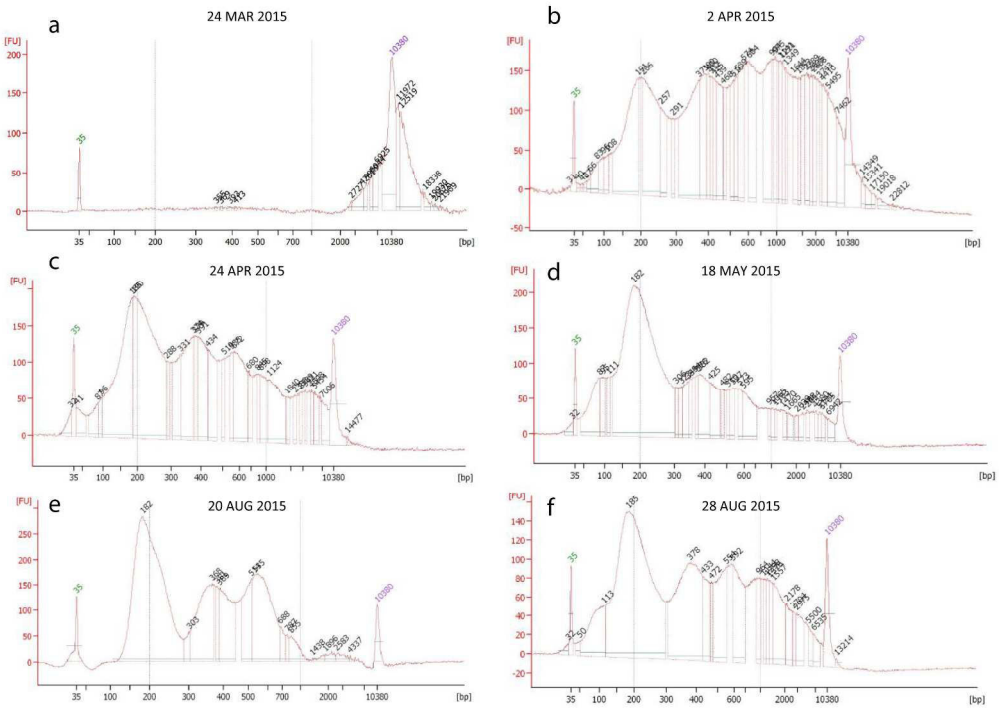

254x190mm (300 x 300 DPI)

Supplementary Figure 2

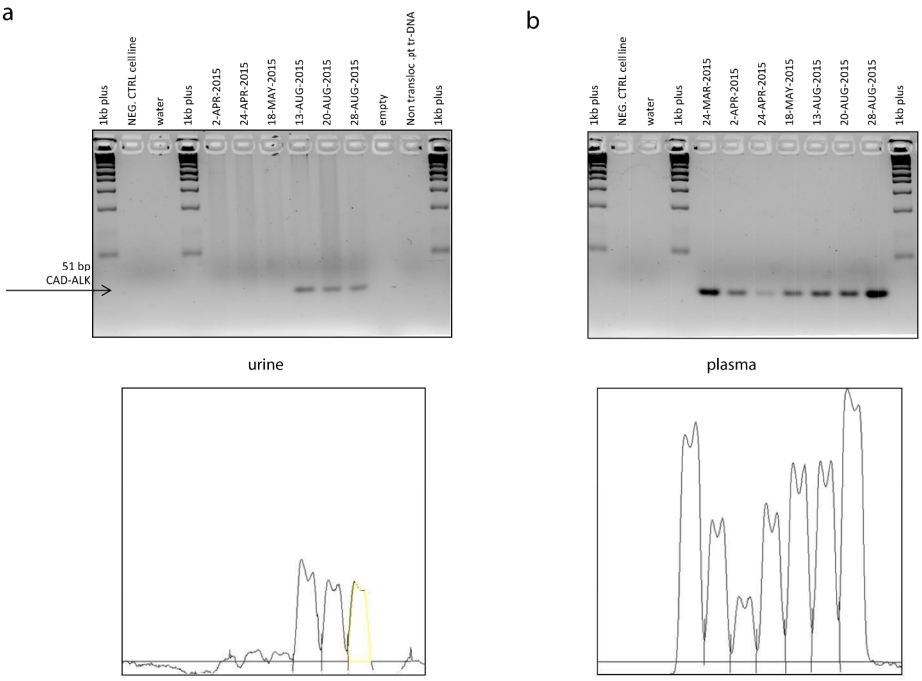

254x190mm (300 x 300 DPI)

Supplementary Figure 3

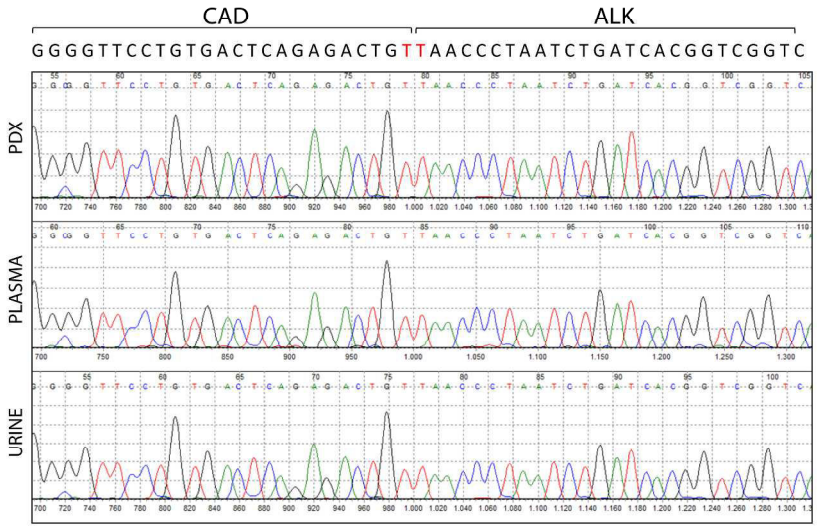

254x190mm (300 x 300 DPI)

Supplementary Figure 4

a

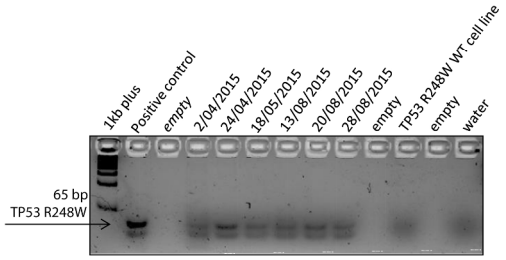

b

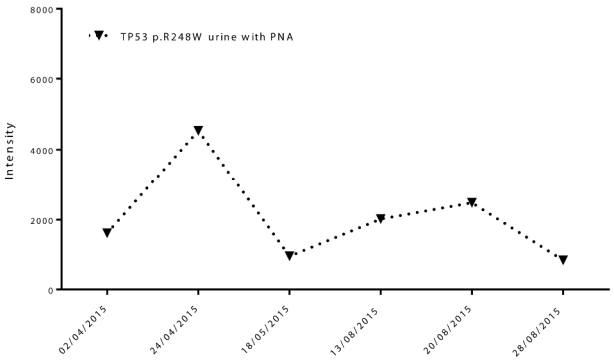

254x190mm (300 x 300 DPI)

Supplementary Table 1

a

Gene Fusions				
Gene	**Transcript**	**Exons caputured**	**Introns captured**	**Analyzed bases**
AES	ENST00000221561	2	1	1538
AKAP13	ENST00000361243	35	35	2444
ALK	ENST00000389048	2,17,19,20	1,16,18,19	207297
BAIAP2L1	ENST00000005260	2	1	38443
BCAN	ENST00000329117	13	13	482
CCDC6	ENST00000263102	1,2,6	1,6	56508
CD74	ENST00000353334	6,7	6,7	2513
CEP85L	ENST00000368491	8	8	1418
EIF3E	ENST00000220849	1	1	6850
ELAVL3	ENST00000359227	2	1	13990
EML4	ENST00000318522	2,6,13,14,15,18,19,20,21	2,6,13,14,15,18,19,20,21	59456
ERC1	ENST00000589028	7,10,12	7,10,12	71757
EZR	ENST00000367075	10	10	948
FGFR3	ENST00000340107	17	17	285
GOLGA5	ENST00000163416	7	7	3455
GOPC	ENST00000368498	8	8	3648
GTF2IRD1	ENST00000265755	7	7	2861
HOOK3	ENST00000307602	11	11	5724
KIF5B	ENST00000302418	15,16,22,23,24	15,16,22,23,24	9032
KLC1	ENST00000348520	9	9	2218
KTN1	ENST00000395314	29	29	2502
LMNA	ENST00000368300	2,10,11	2,10,11	5206
LRIG3	ENST0000037914	16	16	2028
MPRIP	ENST00000395811	21	21	2751
NCOA4	ENST00000578454	7	7	611
NFASC	ENST00000339876	21	21	5618
NTRK1	ENST00000524377	7,10,11,12	6,9,10,11	4366
PCM1	ENST00000325083	29	29	12778
PRKAR1A	ENST00000358598	7	7	2084
PTPRK	ENST00000368226	1,7	1,7	217715
RET	ENST00000340058	8,11,12	7,10,11	3927
ROS1	ENST00000368508	32,34,35,36	31,33,34,35	14191
RSPO2	ENST00000276659	2	1	650
RSPO3	ENST00000356698	2	1	29548
SDC4	ENST00000372733	2,4	2,4	5996
SLC34A2	ENST00000382051	4	4	1924
SMEK2	ENST00000611717	10	10	8991
SPECC1L	ENST00000314328	10	10	8698
STRN	ENST00000263918	3	3	10531
TACC3	ENST00000313288	4,8,11	3,7,10	7496
TBL1XR1	ENST00000457928	9	9	1206
TFG	ENST00000240851	4,5	4,5	7860
TP53	ENST00000620739	8,9,10,11	8,9,10,11	2805
TPM1	ENST00000267996	8	8	8512
TPM3	ENST00000368530	8	8	13830
TPM4	ENST00000300933	5	5	4489
TRIM24	ENST00000343526	9	9	12781
TRIM27	ENST00000377199	3	3	8522
TRIM33	ENST00000358465	14	14	1339
VCL	ENST00000372755	16	16	2177

b

Mutations			
Gene	**Transcript**	**Exons captured**	**Analyzed bases**
APC	All isoforms	All exons	8697
AREG	ENST00000395748	1	496
BRAF	ENST00000288602	15	118
CTNNB1	All isoforms	All exons	2346
EGF	ENST00000265171	1	452
EGFR	ENST00000275493	12	199
EREG	ENST00000244869	1	166
KRAS	ENST00000311936	2,3,4	458
MAP2K1	ENST00000307102	2	210
NRAS	ENST00000369535	2,3	305
PIK3CA	ENST00000263967	10,21	395
PTEN	All isoforms	All exons	1731
TGFA	ENST00000295400	1	248
TP53	All isoforms	All exons	1263

Supplementary T

IRCC-Fusion panel – NGS ANALYSIS
ctDNA baseline entrectinib vs reference genome (hg19)

a

5' Gene Name	5' Coordinate	3' Gene Name	3' Coordinate
ALK	chr2:29447551	CAD	chr2:27463267
CAD	chr2:27463262	ALK	chr2:29447543

Cosmic	Gene	Description	Coordinate	N change	AA change	Variant Effect	% Mutant Reads
641	TP53	Tumor protein p53	chr17:7577539	c.C742T	p.R248W	nonsyn	7.75

IRCC- TARGET panel – NGS ANALYSIS
ctDNA progression vs cfDNA baseline to entrectinib

b

Cosmic	Gene	Description	Coordinate	N change	AA change	Variant Effect	% Mutant Reads
57	ALK	anaplastic lymphoma receptor tyrosine kinase	chr2:29443695	c.C3522G	p.F1174L	nonsyn	1.93237
14	ALK	anaplastic lymphoma receptor tyrosine kinase	chr2:29443697	c.T3520C	p.F1174L	nonsyn	6.08175
11	ALK	anaplastic lymphoma receptor tyrosine kinase	chr2:29443696	c.T3521G	p.F1174C	nonsyn	1.40987
8	ALK	anaplastic lymphoma receptor tyrosine kinase	chr2:29436860	c.T3733G	p.F1245V	nonsyn	1.33753
1	ALK	anaplastic lymphoma receptor tyrosine kinase	chr2:29445450	c.G3383C	p.G1128A	nonsyn	2.83871

Sample	Target	Mutated events	Wild-type events	Fractional Abundance(%)
plasma ctDNA 24-MAR-2015	*TP53* p.R248W	45	425	9.7
	ALK p.F1174L (C>G)	0	332	0.0
	ALK p.F1174L (T>C)	0	366	0.0
	ALK p.F1174C	0	378	0.0
	ALK p.G1128A	1	330	0.1
	ALK p.F1245V	0	331	0.0
plasma ctDNA 2-APR-2015	*TP53* p.R248W	0	247	0.0
	ALK p.F1174L (C>G)	0	183	0.0
	ALK p.F1174L (T>C)	1	205	0.2
	ALK p.F1174C	1	213	0.1
	ALK p.G1128A	0	165	0.0
	ALK p.F1245V	0	171	0.0
plasma ctDNA 24-APR-2015	*TP53* p.R248W	1	186	0.2
	ALK p.F1174L (C>G)	0	167	0.0
	ALK p.F1174L (T>C)	0	153	0.0
	ALK p.F1174C	0	152	0.0
	ALK p.G1128A	0	129	0.0
	ALK p.F1245V	0	135	0.0
plasma ctDNA 18-MAY-2015	*TP53* p.R248W	1	237	0.4
	ALK p.F1174L (C>G)	1	206	1.0
	ALK p.F1174L (T>C)	0	231	0.0
	ALK p.F1174C	0	188	0.0
	ALK p.G1128A	0	154	0.0
	ALK p.F1245V	0	182	0.0
plasma ctDNA 13-AUG-2015	*TP53* p.R248W	181	331	35.8
	ALK p.F1174L (C>G)	19	854	2.1
	ALK p.F1174L (T>C)	53	935	5.5
	ALK p.F1174C	17	927	1.9
	ALK p.G1128A	45	734	5.8
	ALK p.F1245V	11	762	1.6
plasma ctDNA 20-AUG-2015	*TP53* p.R248W	416	1675	20.2
	ALK p.F1174L (C>G)	32	2528	1.4
	ALK p.F1174L (T>C)	132	2600	5.3
	ALK p.F1174C	34	2571	1.4
	ALK p.G1128A	51	1973	2.7
	ALK p.F1245V	21	2098	1.1
plasma ctDNA 28-AUG-2015	*TP53* p.R248W	831	1187	41.4
	ALK p.F1174L (C>G)	60	4274	1.5
	ALK p.F1174L (T>C)	307	4160	7.7
	ALK p.F1174C	74	4388	1.8
	ALK p.G1128A	155	3561	4.5
	ALK p.F1245V	55	3941	1.5